POLITECNICO DI TORINO
Repository ISTITUZIONALE

Functionalized carbon nanotubes tape for energy harvesting from salinity gradients through asymmetric capacitive mixing

Original
Functionalized carbon nanotubes tape for energy harvesting from salinity gradients through asymmetric capacitive mixing / Pedico, A., Seller, F., Blandolino, Y., Martellone, S., Lamberti, A.. - In: RENEWABLE ENERGY. - ISSN 0960-1481. - 258:(2026), pp. 1-8. [10.1016/j.renene.2025.124995]

Availability:
This version is available at: 11583/3005889 since: 2025-12-15T14:03:51Z

Publisher:
Elsevier

Published
DOI:10.1016/j.renene.2025.124995

Terms of use:

This article is made available under terms and conditions as specified in the corresponding bibliographic description in the repository

Publisher copyright

(Article begins on next page)

18 November 2026

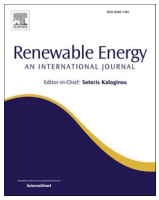
Renewable Energy 258 (2026) 124995



Contents lists available at ScienceDirect

Renewable Energy

journal homepage: www.elsevier.com/locate/renene



Functionalized carbon nanotubes tape for energy harvesting from salinity gradients through asymmetric capacitive mixing

Alessandro Pedico [a,b,*], Francesco Seller [a], Yari Blandolino [a], Simone Martellone [a,c], Andrea Lamberti [a,c]

[a] Politecnico di Torino, Dipartimento di Scienza Applicata e Tecnologia (DISAT), Corso Duca degli Abruzzi, 24, 10129, Torino, Italy
[b] Istituto Nazionale di Ricerca Metrologica, Strada delle Cacce, 91, 10135, Torino, Italy
[c] Istituto Italiano di Tecnologia, Center for Sustainable Future Technologies, Corso Trento, 21, 10129, Torino, Italy

ARTICLE INFO

Keywords:
Capacitive mixing
Carbon nanotubes
Energy harvesting
Blue energy

ABSTRACT

In this work, we investigated the possibility of using a commercial tape entirely made of continuous carbon nanotubes (CNTs) for blue energy harvesting application. The tape was used to build the electrodes of a device harvesting energy from salinity gradient based on the capacitive mixing (CapMix) technique. The tape was used as it is or functionalized to enhance its storage properties and to obtain an asymmetric device. The electrodes underwent a full set of electrochemical characterizations to test the impact of the functionalization. Thanks to high electrical conductivity, remarkable specific capacitance and good chemical stability, the tape acted both as active material and current collector, eliminating the need for metallic current collectors, reducing the mass of the system and avoiding possible corrosion of the metals due to close contact with saline solutions. This approach provided a simple and easily scalable device able to produce electrical power from the mixing of two solutions at different salinities. The achieved power output stands at 75 μW m^{-2} in artificial seawater/freshwater and 1.2 mW m^{-2} in artificial Mediterranean brine/seawater. These results contribute to the broader understanding of energy harvesting from salinity gradients, extending the technological application of CNT tape across the renewable energy field.

1. Introduction

The demand for energy is continuously increasing worldwide. The world population growth, the increasing number of facilities and the electrified mobility put a challenge to researchers to provide new materials and technologies to produce energy in a more efficient and economical way. The growth of developing countries goes in parallel with an increasing demand for energy. Developing countries currently use more than half of the world's energy, with their demand for energy virtually doubled in the last two decades and expected to keep increasing [1]. In order to fulfill this necessity, new energy sources must be found, since traditional ones (oil, natural gas, coal, etc …) are not sustainable for the habitat of our planet: climate change is the global reminder for choosing the green path. Energy production must come from renewable sources like solar, wind and biomass, but also new solutions are under investigation. An example is the so called 'Blue Energy', which refers to all types of techniques that are able to harvest energy from the sea and the water in general. A particular example is the Salinity Gradient Energy (or Salinity Gradient Power), a free energy which is dissipated in the form of heat when mixing two solutions with different salinity. In nature, this commonly happens when a river flows into the sea and results in a dissipation of free energy. In order to harvest this energy, it is necessary to control the mixing of the two solutions (seawater and freshwater), converting this free mixing energy into another form of energy that can be exploited for human activities. This is a completely green energy source, since it is renewable and does not produce any carbon byproducts. Another advantage is that the power production from salinity gradients is continuous (while solar and wind, for example, suffer from production discontinuity). For these reasons, in the last decades, efforts have been spent trying to harvest energy from salinity gradients and different techniques have been investigated, the most important being pressure-retarded osmosis [2], reverse electrodialysis [3], and capacitive mixing [4]. The reason is that, considering all the rivers on Earth, the amount of power at stake is of the order of 1 TW, making this source very promising [5].

This Salinity Gradient Energy can be harvested using different

* Corresponding author. Istituto Nazionale di Ricerca Metrologica, Strada delle Cacce, 91, 10135, Torino, Italy.
E-mail address: a.pedico@inrim.it (A. Pedico).

https://doi.org/10.1016/j.renene.2025.124995
Received 10 January 2025; Received in revised form 5 December 2025; Accepted 6 December 2025
Available online 6 December 2025
0960-1481/© 2025 The Authors. Published by Elsevier Ltd. This is an open access article under the CC BY license (http://creativecommons.org/licenses/by/4.0/).

techniques, able to convert this energy into mechanical or electrical energy. The most famous techniques are Pressure Retarded Osmosis (PRO), Reverse Electrodialysis (RED) and Capacitive Mixing (CapMix). The working principle of the PRO is based on the presence of semi-permeable membranes which allow the passage of water from freshwater to seawater, generating an osmotic pressure that is used to pressurize the seawater and move a turbine, converting the mixing energy in mechanical energy and then in electrical energy. The RED instead exploits ion exchange membranes to control the movement of ions from the seawater to the freshwater. Alternating the fluxes of freshwater and seawater in a stack of ion exchange membranes, it is possible to create a net ion current to generate electrical energy. The working principle of CapMix hinges on supercapacitor technology. The cell, composed of two porous electrodes, is designed in such a way that an electrolyte solution can be flushed between them. In CapMix, the controlled mixing of two solutions is used to harvest energy converting it in electric power in an external circuit.

To harvest energy through the CapMix, a cycle made of four steps is required. In the first step, in open circuit condition, the space between the electrodes is filled with a highly concentrated solution. In the second step, an external power source provides electrical energy to charge the electrodes up to a fixed voltage. In the third step, the external power source is disconnected and the solution is replaced with a less concentrated solution. In this step, the injection of low salinity water is causing an expansion of the electrical double layer previously formed on the surface of the electrodes. This expansion, located in the diffuse part of the electrical double layer, is responsible for a voltage rise of the cell. In the final step, the device is discharged on a load to harvest the energy obtained from the spontaneous voltage rise and the process is repeated.

Firstly proposed by Brogioli in 2009 [6], this technique was further studied in the past decade to improve its performance, obtaining results which proved the potential of this technique, boosting the output power by correctly tuning the experimental parameters [7] or by modifying the surface chemistry of the active materials [8,9]. Over the years, three different working principles have been investigated so far for this technique, namely, Capacitive Double Layer Expansion [10], Capacitive Donnan Potential [11] and Mixing Entropy Battery [12], respectively based on the variation upon salinity change of the electric double layer capacity, on the variation of the Donnan potential of ion exchange membranes, and on the variation of the electrochemical energy of intercalated ions.

CapMix was initially thought to harvest energy where two natural gradients are present, i.e. where rivers meet the ocean, but that's not the only possibility. Human activity is responsible for the production of brines, which are solutions with a salt concentration higher than seawater. Those solutions are usually a waste product that requires dedicated management. They can come from salterns or desalination plants and undergo a strict discharge regulation because they are dangerous for the aquatic environment. However, their high salt content can become a resource. Indeed, their chemical energy can be converted to electricity when mixing them with a lower salinity source, like seawater. This process of mixing is already commonly employed industrially, without recovering this energy, that is wasted as heat. In this context, the CapMix technology is attracting the interest of the scientific community, with reports on membrane-free devices [13], membrane-based devices [14] and hybrid combinations [15].

While the feasibility of energy production from salinity gradients has already been demonstrated [16], the CapMix technology is not yet ready for real-world operation. One of the main reasons is that electrode materials lack the necessary, yet challenging, combination of physico-chemical properties. As deeply discussed by Lobato et al. [17], these materials must have a large ion-accessible specific surface area for high electrosorption capacity, combined with high ion mobility and excellent electrochemical stability. Crucially, they require high electronic conductivity to minimize energy losses. Also, the pore size of these materials is a crucial parameter, as discussed by Nasir et al. [18]. Finally, the electrode materials must be scalable and cost-effective. For this reason, most of the electrodes reported are carbon-based, as recently documented by Han et al. [19], describing the use of chemically modified activated carbons for energy extraction from salinity gradients.

Carbon nanotubes (CNTs)-based nanomaterials are widely used for the development of energy harvesting devices [20]. They are commonly used as current collectors integrated in triboelectric [21] or piezoelectric [22] materials, or in thermoelectric [23] and photermal devices [24]. The CNTs find application in the field of energy harvesting thanks to the possibility of exploiting different phenomena to harvest energy using CNTs themselves as active material [25]. Like all the sp^2 hybridized carbon materials, the CNTs form weak interactions with water [26,27], polar organic solvents [28], and with ions present in solution [29]. The functionalization of CNTs is also widely studied to improve their wettability, exploiting chemical treatments in acids to both induce a certain degree of functionalization and increase the porosity of the surface [30,31]. Despite that, few promising works can be found in literature reporting the use of CNTs as active material for CapMix applications in salty water [32]. In most cases CNTs are used as additives rather than active materials [33].

CNTs offer distinct advantages over other carbon-based electrode materials. Compared to activated carbon, which is cost-effective and has a high surface area, CNTs typically provide superior electrical conductivity and a more readily accessible surface area due to their tubular structure and defined porosity [34]. Also, activated carbons require the presence of a current collector, while CNTs can act both as active material and current collector. When compared to graphene and its derivatives, CNTs can exhibit comparable or higher electrical conductivity, especially on large surface area in which graphene-based materials show defectiveness, discontinuity and restacking of sheets, which limits ion accessibility and reduces specific capacitance [35]. Finally, CNTs have excellent mechanical strength and flexibility, surpassing many polymer-based electrodes which can be limited by poorer chemical and thermal stability. Also, the alignment and controllable structure of CNTs allow for enhanced ion diffusion and better rate capability.

In this work, a tape made of CNT yarn has been investigated for the first time as a possible CapMix electrode for energy recovery from salt gradients. Several chemical and electrochemical functionalizations are proposed and compared to improve the material performance for this application.

2. Material and methods

2.1. CNT electrode preparation

CNT tape (Galvorn, width 1 cm, thickness 20 μm, linear density 0.27 g m^{-1}, conductivity 5 MS m^{-1}, from Dexmat) was used as electrode for CapMix application. The CNT tape was cut to the desired length and an electric contact was made with a titanium grid, surrounded by an adhesive polyimide tape around the contact point. This electrode was used as it was or treated to activate the CNT surface and tune its properties. Chemical and electrochemical activations were performed to tune the surface functional groups and improve the surface area and the specific capacitance. A first activation process was developed starting from the one used by Serrapede et al. on a CNT-based material produced in form of yarn [36]. The CNT tape was immersed for 2 h in a 1 M potassium hydroxide (KOH, 90 % purity, Merck) solution at 60 °C and then washed with deionized water (Direct-Q 3 UV, Merck Millipore). Successively, an electrochemical activation followed, in which the CNT tape was subjected to a potential cycling, linearly sweeping the potential applied back and forth from −0.06 V to +1.84 V vs Ag/AgCl at a speed of 10 mV s^{-1} in a 4 M nitric acid (HNO_3, 70 %, Merck) solution for 2 times. This activation allows to break the carbon-carbon bonds of the nanotubes present in the CNT tape and to defect the lattice, increasing the porosity while contemporarily adding functional groups to the surface. The number of activation cycles is crucial and it was chosen to maximize the

capacitive behavior while simultaneously limiting the loss in conductivity of the material. While electrochemical activations can break the carbon bonds of graphitic lattices and allow to monitor the health of the electrode during activation, chemical activations allow materials to be activated with reduced electrical energy consumption and are more easily scalable. Pristine CNT tape is hydrophobic and is more easily wetted by organic solvents. A second kind of activation process was performed immersing the CNT tape for 2 h in a 3 % v/v solution of HNO_3 in ethanol (>99 % purity, anhydrous, Merck), washing with deionized water at the end. This mixture of ethanol and nitric acid, commonly known as "Nital", is a chemical reagent used in steel polishing to highlight the different iron-carbon phases within it. This reagent was chosen to provide a faster and easier, yet milder activation of the CNT tape. To distinguish the different materials, from now on, the pristine CNT tape is simply called CNT, the result of the first activation is called CNT_KOH and, analogously, CNT_EtOH is the result of the second activation.

2.2. NaCl solution preparation

The sodium chloride (NaCl, anhydrous, ≥99 % purity, Merck) was dissolved in deionized water to obtain solutions of 600 mM and 10 mM for artificial seawater and freshwater, respectively. For electrochemical characterizations, a 1 M solution was prepared.

2.3. Brine preparation

The brine was prepared mimicking the composition of the Mediterranean seawater. This composition was obtained combing the data reported in different studies [37–41]. NaCl, magnesium chloride ($MgCl_2$, anhydrous, ≥98 % purity, Merck), sodium sulfate (Na_2SO_4, anhydrous, ≥99 % purity, Merck), potassium sulfate (K_2SO_4, ≥99 % purity, Merck), calcium chloride ($CaCl_2$, dihydrate, ≥99 % purity, Merck), sodium bicarbonate ($NaHCO_3$, ≥99.7 % purity, Merck), sodium bromide (NaBr, ≥99 % purity, Merck), strontium bromide ($SrBr_2$, hexahydrate, ≥99 % purity, Merck), boric acid (H_3BO_3, ≥99.5 % purity, Merck), sodium nitrate ($NaNO_3$, ≥99 % purity, Merck), sodium fluoride (NaF, ≥99 % purity, Merck) and lithium chloride (LiCl, ≥99 % purity, Merck) were dissolved in deionized water to obtain a brine with a salinity 5 times higher than seawater (Table 1). A diluted brine was obtained adding deionized H_2O to the brine in a 1:4 dilution ratio, to obtain an artificial seawater useful for CapMix experiments.

2.4. Cell design

The cell used for CapMix measurement was a homemade cell, composed of two planar half-cells. The material of the cell was poly (methyl methacrylate). This material was chosen because of its transparency, good rigidity, low cost, chemical compatibility with salinity solutions and ease of milling. The CAD file of the cell was generated with SolidWorks and then provided to the CNC milling machine (MDX-50, Roland).

Table 1
Simulated brine composition.

SALT	QUANTITY	CONCENTRATION
NaCl	123.2 g	2.1 M
$MgCl_2$	25.2 g	265 mM
Na_2SO_4	16.25 g	114 mM
K_2SO_4	4.35 g	25 mM
$CaCl_2$	1.26 g	11.4 mM
$NaHCO_3$	1.0 g	12 mM
NaBr	353 mg	3.4 mM
$SrBr_2$	135 mg	0.5 mM
H_3BO_3	128 mg	2 mM
$NaNO_3$	26 mg	0.3 mM
NaF	11 mg	0.25 mM
LiCl	5.3 mg	0.1 mM

The top of the cell (Fig. 1a) was 40 mm long and 30 mm wide, while its height was 5 mm. There were four holes at the angles that had a diameter of 3.5 mm and were intended to host the screws that hold the two parts together. Three other holes with the same diameter were destined to be the inlets and the outlet. Two more openings (1 cm long and 1 mm wide) were created to let the two electrodes enter the device: they were separated by a distance of 1 cm, allowing for an electrode area of 1 cm^2. A channel connected the inlets with the outlet and had a depth of 1 mm. A barrier (0.5 mm high and 0.5 mm wide) was created around the channel to improve the adhesion with the bottom part and avoid any liquid dispersion. The bottom of the cell (Fig. 1b) was 40 mm long and 30 mm wide, while its height was 3 mm. There were four holes (3.5 mm diameter) in the same spots of the top half for the screws. A channel (2.5 mm wide) with the same shape as the barrier of the top half-cell was

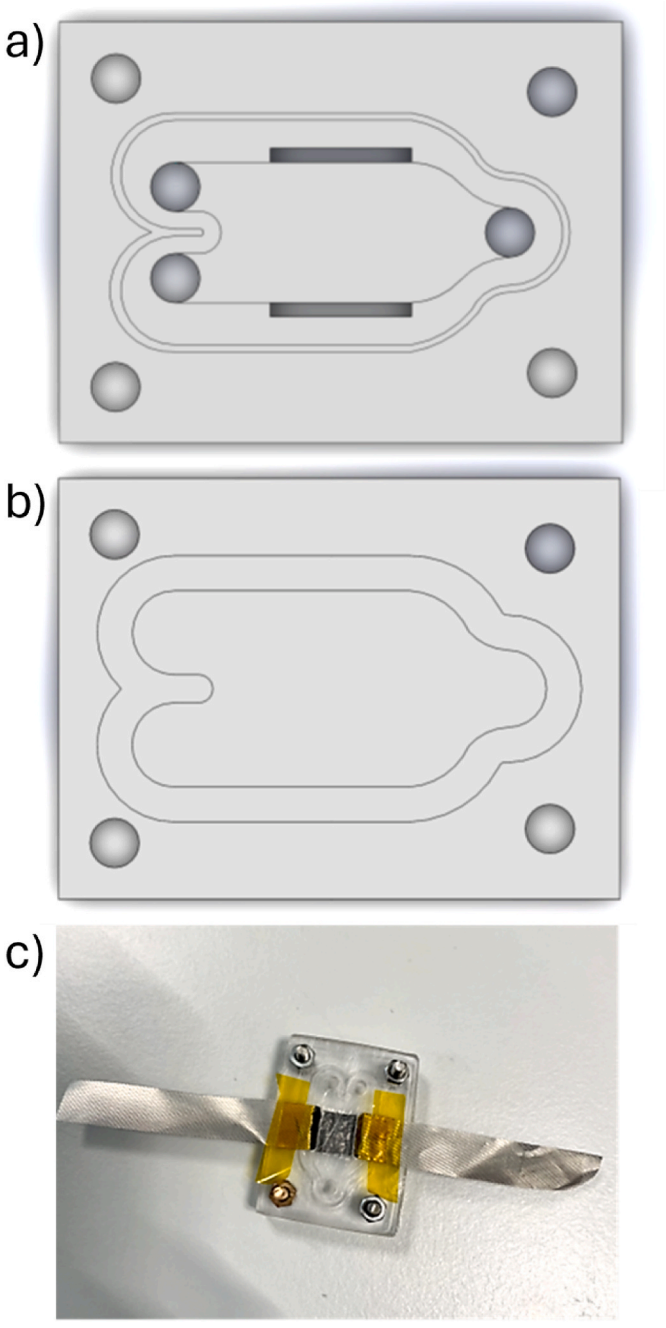


Fig. 1. a) Top view of the CapMix cell. Scale of 1.5:1. b) Bottom view of the CapMix cell. Scale of 1.5:1. c) Mounted cell with electrodes.

created. Inside this channel, polydimethylsiloxane was used as transparent, soft and inert sealing. When the cell was closed, the barrier came in contact with it, avoiding any leakage of the solution.

2.5. Characterization techniques

Electron microscopy characterization was carried out with a Field-Emission Scanning Electron Microscope (FESEM Supra 40, manufactured by Zeiss) equipped with a Si(Li) detector (Oxford Instruments) for Energy-Dispersive X-ray (EDX) spectroscopy.

The electrochemical measurements were performed with a VMP3 potentiostat provided by Bio-Logic. This instrument offers a potential range of ±10 V, a maximum current of 400 mA, with a resolution of 50 μV and 760 pA. The accuracy is declared to be <0.1 % of the full-scale range. The electrometer has an input impedance greater than 1 TΩ, a capacitance of less than 20 pF, and a bias current lower than 5 pA.

Specific surface area was measured at 77 K by N_2 sorption porosimetry using ASAP2020 Plus, Micromeritics. Before the analysis, the sample was heated to 150 °C under vacuum for 110 min, with a ramp rate of 10 °C min^{-1} to remove adsorbed moisture and any residual organic contaminants.

2.6. Electrochemical methods

Apart from the CapMix cycles, all the electrochemical characterizations and activations were performed in a 3-electrode configuration, with the aim of characterizing key parameters of the electrode materials that will directly influence their CapMix performance (like specific capacitance, internal resistance, etc.). The reference was an Ag/AgCl 3 M KCl electrode. The working electrode was produced as previously explained, while the counter electrode was prepared by mixing 85 % wt. activated carbon (YP-50F, MTI Corporation), 5 % wt. carbon black (Timical C65, Imerys) and 10 % wt. polytetrafluoroethylene (60 % wt. dispersion in H_2O, Merck) in ethanol. The slurry was dried until it got the consistency of a dough and then flattened over a titanium grid, resulting in a dense and thick layer. The layer was cut in the desired shape and dried at 60 °C overnight. This preparation resulted in a 1 mm thick stand-alone electrode.

Before any electrochemical characterization, the cell was rested at open circuit conditions for about 2 h in a NaCl 1 M solution. The potentiostatic impedance spectroscopy was performed by applying a sinusoidal signal with an amplitude of 10 mV and a frequency ranging from 1 MHz to 10 mHz. Cyclic voltammetries were performed at a scan rate of 5 mV s^{-1}, between 0 V vs open circuit potential (OCP) and +0.5/-0.5 V vs OCP, with steps of 100 mV. Anodic and cathodic scans were performed on different electrodes, in order to decouple the measurements. During each step, the cyclic voltammetry was repeated at least 50 times. Galvanostatic charge-discharge technique was used to investigate the stability of the CNT tape. All these measurements were performed in a NaCl 1 M solution.

For each material under investigation, the voltage rise as function of the applied potential was evaluated. The adopted procedure included 5 min of constant voltage (from 0 V vs OCP up the maximum of the potential window, with steps of 100 mV) in concentrated solution, then some minutes in open circuit conditions, during which the concentrated solution was replaced by the diluted one. In this second step the voltage rise was measured. When the potential had reached a plateau, the freshwater was removed, and the seawater was poured in. The measurement was then repeated a total of 5 times to ensure reproducibility and check stability.

The CapMix was performed following the standard 4-steps CapMix cycle. The first step in which the cell was charged in high salinity solution, a second step in which the device was left in open circuit condition while the solution was switched to low salinity, then a discharge step and finally another open circuit step in which the solution was switched back to high salinity. A gear pump (Analog Gear Pump, Masterflex) guaranteed a constant and homogeneous water flux, providing a fast and smooth change of the whole volume of solution inside the CapMix cell. The charge and discharge steps were performed following a constant current method. The device was left 1 h in open circuit condition in high salinity solution. After this time, the open circuit voltage (OCV) was set as operating voltage at which the device was set to work, i.e. while cycling, the cell was always charged and discharged up to that OCV value. The harvested energy was evaluated as the difference between the energy recovered during the discharge step and the energy spent to charge the device during the charge step, both evaluated as the integral over time of the instant electrical power. The power output was evaluated as the energy harvested in one cycle divided by the total time duration of the same cycle. The energy extraction efficiency was evaluated as the ratio of the extracted energy in one cycle and the theoretical maximum energy that can be extracted from the mixing of the two solutions.

3. Results and discussion

3.1. Material characterization

Electron microscopy was employed to study the morphology of the CNT samples, in order to check if the morphology of the CNT tape was affected by the treatments. Fig. 2 reports a comparison of the active materials tested. The structure of the CNT is shown in Fig. 2a, where it is possible to appreciate a quite flat and ordered surface, with most of the bundles of nanotubes sticking together. Fig. 2b shows how the surface of the CNT_KOH is drastically changed, with the bundles spread open and more wavy. Interestingly, from the morphological point of view, the treatment seems to affect only the cohesion of the nanotubes along their length, thus spreading them from their original packed structure, without damaging them on the perpendicular direction. In Fig. 2c it is possible to observe the CNT_EtOH sample, having a morphology less ordered than CNT, but not as much as CNT_KOH.

The electrochemical characterizations were implemented in order to evaluate the potentialities of these materials for CapMix application, investigating some key parameters such as capacitance, operative voltage windows and equivalent series resistance.

Electrochemical impedance spectroscopy was initially performed, followed by cyclic voltammetry. For all the samples (Fig. 3a), it is possible to observe a typical capacitive behavior. No appreciable charge transfer can be observed. While CNT and CNT_EtOH have similar behavior, the CNT_KOH is more resistive. The internal resistance is affected by three main contributions: the solution conductivity (negligible in 1 M NaCl), the quality of the contacts and the electrical resistivity of the materials. The length of the electrodes and the way they were contacted are the same. Since the pristine CNT was the least wettable and exhibited a low internal resistance, the higher resistance of the CNT_KOH can be reasonably addressed to the functionalization process, adding defects and oxygen groups that lower the electronic conductivity.

The cyclic voltammetry curves of CNT, CNT_EtOH and CNT_KOH are shown in Fig. 3b, c and 3d, respectively. The CNT has higher specific capacitance in the cathodic window (Fig. 3e) with a coulombic efficiency always above 90 % (Fig. 3f). The CNT_EtOH shows an opposite behavior, having a higher specific capacitance in the anodic window, while keeping the coulombic efficiency always higher than 95 %. The CNT_KOH shows the lowest specific capacitance in the cathodic window, while having the lowest coulombic efficiency at any voltage window. Moreover, in the anodic window, the coulombic efficiency drastically drops, starting from 0.4 V, whereas the specific capacitance increases exponentially, with the cyclic voltammetry clearly showing signs of irreversible redox reactions happening. The results of the CNT_KOH activation are comparable with the ones reported by Serrapede et al. [36]: The overall potential window decreases in width, due to the formation of surface functional groups that catalyze water splitting

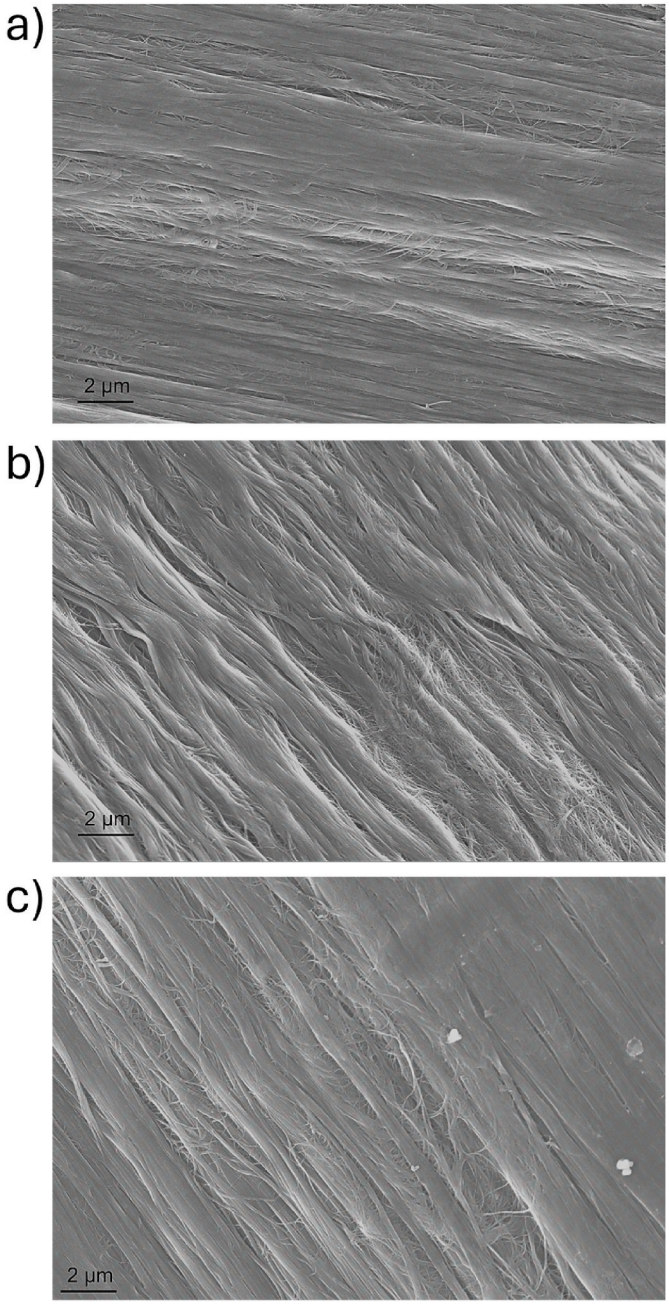


Fig. 2. SEM images of the active materials: a) CNT b) CNT_KOH c) CNT_EtOH.

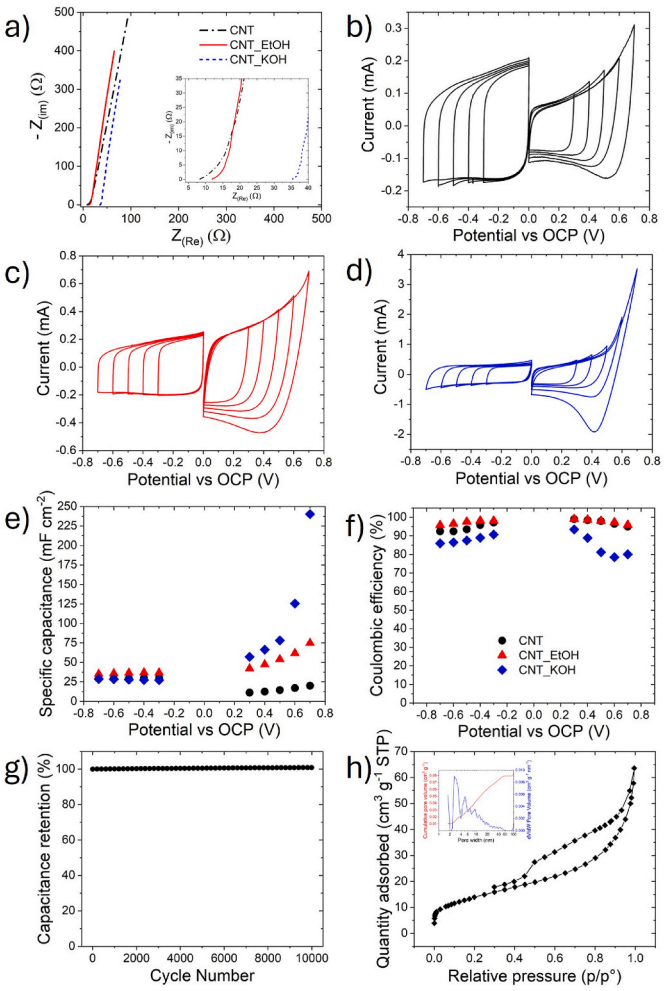


Fig. 3. Electrochemical characterizations. a) Impedance spectroscopy. b) Cyclic voltammetry of CNT. c) Cyclic voltammetry of CNT_EtOH. d) Cyclic voltammetry of CNT_KOH. e) Specific capacitance. f) Coulombic efficiency. g) Capacitance retention of CNT. h) Investigation of CNT porosity. Main: BET results. Inset: NLDFT analysis.

at lower potentials. At the same time, pseudocapacitive peaks are observed, which however occur in the anodic window of the material. This behavior is associated with the neutral pH at which measurements are performed. The protonation of oxygen-based functional groups of graphitic lattices shifts to more anodic potentials at neutral pH, as is known in the case of carbon fibers [42] and more generally in the case of surface functional groups of carbonaceous materials [43].

The capacitance retention of the CNT (Fig. 3g) was evaluated using a current density of 2 μA cm^{-2}. As can be clearly observed, this material proved to be highly stable over ten thousand cycles. The specific surface area of the CNT was determined by nitrogen sorption porosimetry. The N_2 adsorption-desorption isotherm (Fig. 3h) displays a typical H3 type hysteresis loop according to IUPAC classification. This type of loop can originate from non-rigid clusters of plate-like particles, or from macropores that are only partially filled with pores condensate [44]. A wide distribution of pore size is typical of this kind of hysteresis. The limited nitrogen uptake at very low relative pressure confirms that microporosity is not a major contributor to the total surface area. The gradual increase of the adsorption branch in the 0-2 – 0.8 p/p° range suggests a broad distribution of mesopore widths. This interpretation is consistent with the Non-Local Density Functional Theory analysis (Fig. 3h inset). The cumulative pore volume increases steadily about 3–50 nm, highlighting the contribution of a wide spectrum of mesopores to the overall porosity. A plateau is reached near 60 nm, indicating that pores wider than this value are not significantly present. The specific surface area obtained from the single point adsorption method at 0.95 p/p° is 48.72 m^2 g^{-1}, in agreement with the BET surface area (49.01 ± 0.45 m^2 g^{-1}).

In order to select the optimal coupling between electrodes, the voltage rise was considered as a key parameter. Fig. 4 reports the voltage gain of the different electrodes as function of the applied voltage and the spontaneous potential, in NaCl and brine solutions.

Fig. 4a shows the potential rise in NaCl solution as function of the applied potential. The three materials have a very similar behavior, with CNT_KOH having a higher potential rise for any applied potential, reaching up to 64 mV. Looking at their potential rise at their spontaneous potential (Fig. 4b), it is interesting to note that the couple CNT_KOH (positive electrode) and CNT_EtOH (negative electrode) can be a good choice in a NaCl environment, providing a voltage rise of roughly 30 mV with a voltage difference of only 100 mV. The materials

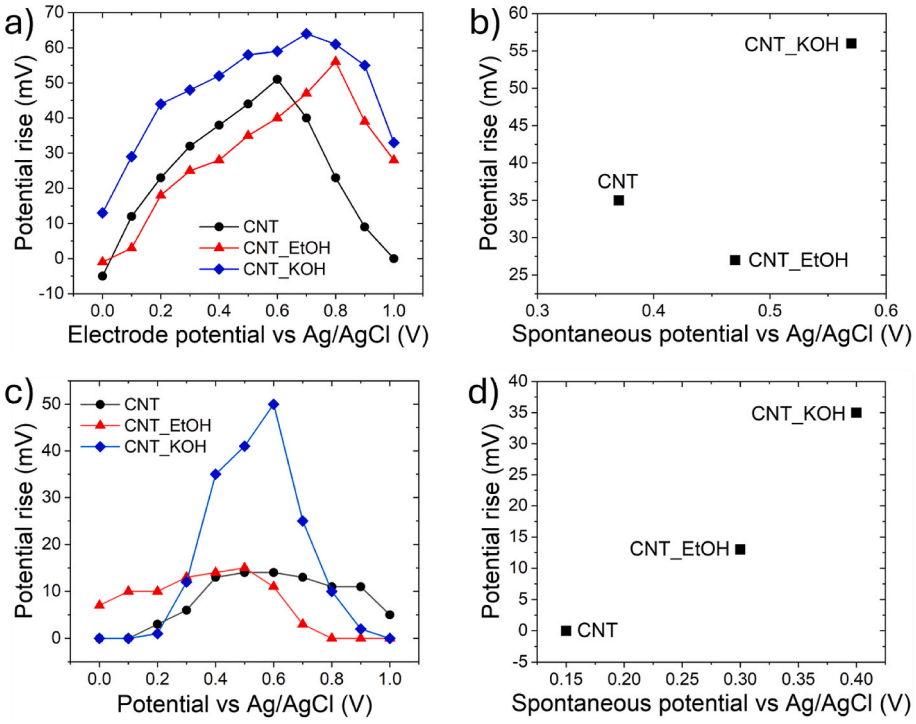


Fig. 4. Voltage gain of different electrodes as function of the: a) electrode potential (NaCl) b) spontaneous potential (NaCl) c) electrode potential (brine) d) spontaneous potential (brine).

show a completely different behavior of their potential rise in brine solution (Fig. 4c). The CNT and CNT_EtOH have specular behavior with respect to the potential applied, however none of them can provide a potential rise higher than 15 mV. On the contrary, the CNT_KOH can outclass their performance, reaching up to 50 mV, but only in a small portion of the curve. This effect is linked to the electrochemical functionalization, affecting the number and the chemistry of the active sites on the surface of the CNT_KOH. This translates into a different formation of the electrical double layer and a different response to the chemical environment, positively affecting the voltage rise in presence of high

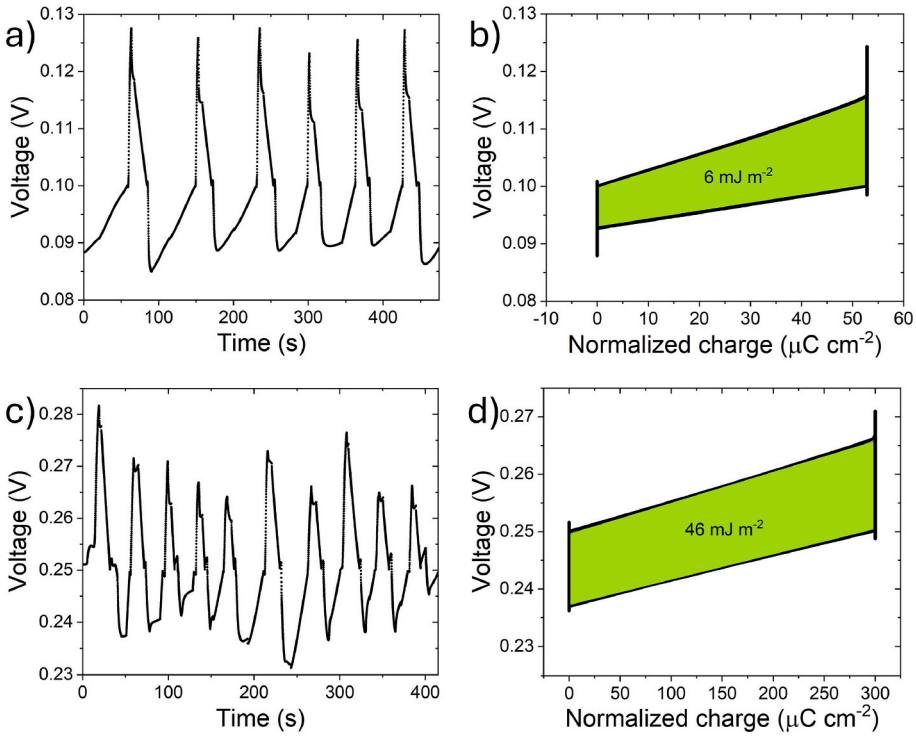


Fig. 5. CapMix results. a) Cycles performed with seawater and freshwater, using CNT_KOH and CNT_EtOH as electrodes. b) Mean energy density per cycle mixing seawater and freshwater. c) Cycles performed with brine and seawater, using CNT_KOH and CNT as electrodes. d) Mean energy density per cycle mixing brine and seawater.

salinity and competing ions. Considering the spontaneous potential of these materials in brine solution (Fig. 4d), it turns out that CNT has no potential rise at its spontaneous potential, requiring an applied positive potential to show just a poor potential rise. On the contrary, the CNT_EtOH keeps a constant low potential rise around 13 mV at its spontaneous potential and also up to a potential applied of ±300 mV. Instead, the spontaneous potential of the CNT_KOH falls in a region of the curve where the material shows a remarkable potential rise. For this reason, the couple CNT_KOH (positive electrode) and CNT (negative electrode) can be a good choice in a brine environment, providing a voltage rise of roughly 35 mV with a voltage difference of 250 mV.

3.2. Capacitive mixing

The experiments were performed using a water flux of 0.1 ml s^{-1} for all the solutions. The operating voltage was set according to the electrochemical characterizations, i.e. 100 mV for seawater/freshwater and 250 mV for brine/seawater. The electrodes were CNT_KOH and CNT_EtOH for the first set of solutions, CNT_KOH and CNT for the second set. The current density for both charge and discharge steps was 2 μA cm^{-2} in the first case and was 30 μA cm^{-2} in the latter.

Fig. 5a shows that the device can work properly at the set voltage, with each cycle in artificial seawater/freshwater lasting ~80 s. The amount of harvested energy per cycle is 6 ± 1 mJ m^{-2} (Fig. 5b). The power output is 75 ± 12 μW m^{-2}. The energy extraction efficiency is approximately 0.3 %. The cycles performed in brine/seawater, instead, were much faster, requiring only ~40 s (Fig. 5c). The amount of harvested energy per cycle is 46 ± 3 mJ m^{-2} (Fig. 5b). The power output is 1.2 ± 0.1 mW m^{-2}. The energy extraction efficiency is around 5 %.

By moving from the seawater/freshwater configuration to the brine/seawater, the energy density, the power density and the energy extraction efficiency increase, as expected. This is the result of the superposition of many complex phenomena like the chemical energy of the solutions and the electrochemical properties of the materials, but, from an electrical point of view, it can be directly addressed to the higher voltage at which the device operates, which provides higher energy density, and the shorter duration of the cycles, which results in higher output power density.

Direct comparison of these results to what is present in literature is not a simple task, since there are no other works on CapMix with CNT tape. In 2014, Liu et al. tested a CNT yarn for CapMix application [32], and they scaled up the system a couple of years later [45]. They used a CNT yarn of ~500 μm in diameter, composed of 370 fibers and coated with ion exchange membranes. In their tests, they obtained a power output of 15 μW g^{-1} in artificial seawater/freshwater, without flushing the water, but rather dipping the cell in the two different solutions. Moreover, for their calculations, they did not consider the mass of the ion exchange membranes, which are strongly contributing to the performance of the device allowing the operation of the cell around 0 V. However, at the best of our knowledge, this example is one of the closest to our study, at least in terms of materials and solutions. Considering the mass density of the CNT tape, our results can be expressed as 2.7 μW g^{-1} in artificial seawater/freshwater. While being slightly lower than what obtained by Liu et al., this is still a great result, considering the scalability and the simplicity of the system, made of a single element (the CNT tape), without costly and resistive ion exchange membranes, which are also subjected to fouling. Unfortunately, this example taken from literature does not allow us to compare the energy density and the power output of the two systems in terms of geometrical area, which is the key parameter when considering scalability. Finally, concerning the energy harvested from brines, there are no studies reporting the use of CTNs.

Considering a general overview of the CapMix scenario, the research is focusing on different materials and configuration (purely capacitive or redox materials [46], ion exchange membranes [47], planar or fancy geometries and flowing electrodes [48], different salinity gradients [4], …). The best performing devices are able to produce a power output of the order of tens of mW m^{-2} [49], but often with complex setup and materials that are not scalable. On a higher level, there are also studies reporting the efforts to push this technology to a more mature level, injecting the electrical energy produced into an external storage or directly to the AC grid [50]. In this scenario, even though higher power output can be found, we believe that our results are interesting for the simplicity and scalability of the device, together with its interesting application to the brine case.

4. Conclusions

This study marks a significant milestone as it introduces, for the first time, the utilization of carbon nanotube tape in Capacitive Mixing experiments, demonstrating its effectiveness in harvesting energy from salinity gradients, using seawater and Mediterranean brine as more concentrated solutions. CNTs are commonly used starting from their dispersed form, often mixed with other materials to obtain a solid disordered matrix suitable for an electrode. In this work, we propose their use in the form of a tape totally made of CNTs, thus not requiring any binding agent nor current collector to build the electrodes. The investigated device comprises two CNT tape electrodes, as they are or functionalized, inserted in a homemade microfluidic cell. Comprehensive electrochemical characterizations have underscored the advantageous impact of the functionalization of CNT. This approach provided a simple device whose performance matches the expectation, successfully producing electrical power from the mixing of two solutions at different salinity. The achieved power output stands at 75 μW m^{-2} in artificial seawater/freshwater and 1.2 mW m^{-2} in artificial Mediterranean brine/seawater. To further enhance the technology, future endeavors will concentrate on larger area devices to verify the scalability. At this stage, the cost of the device is entirely traceable to CNT, accounting for 99 % of the total. At the actual price, the cost of the CNT tape is around 1.3 $ cm^{-2}, compared to the cell and the chemical and electrochemical treatments, which together are approximately 0.03 $ cm^{-2}. Therefore, while market availability and price lowering are essential to foresee any feasibility in scalability, any kind of treatment to improve the performance is perfectly justified. The CapMix perspective will also drive ongoing research, focusing on refining the overall process and exploring novel functionalization as well as ion exchange polymeric coatings. Finally, real solutions (both seawater and brine) will be employed to test the efficiency of the system in a real-case scenario. These advancements will contribute to the broader understanding of energy harvesting from salinity gradients and to the application of CNT tape to a wider technological landscape.

CRediT authorship contribution statement

Alessandro Pedico: Writing – review & editing, Writing – original draft, Visualization, Validation, Methodology, Investigation, Formal analysis, Data curation, Conceptualization. **Francesco Seller:** Writing – review & editing, Writing – original draft, Investigation, Formal analysis, Data curation. **Yari Blandolino:** Investigation. **Simone Martellone:** Writing – review & editing, Investigation, Formal analysis, Data curation. **Andrea Lamberti:** Writing – review & editing, Supervision, Resources, Funding acquisition.

Declaration of competing interest

The authors declare that they have no known competing financial interests or personal relationships that could have appeared to influence the work reported in this paper.

Acknowledgment

This result is part of a project that has received co-funding from the European Research Council (ERC) under the European Union's ERC

Starting Grant. Grant agreement “CO2CAP” No. 949916.

This result is part of a project co-funded by the European Union - NextGenerationEU under the National Recovery and Resilience Plan (NRRP), Mission 04 Component 2 Investment 3.1 | Project Code: IR0000027 - CUP: B33C22000710006 - iENTRANCE@ENL: Infrastructure for Energy TRAnsition aNd Circular Economy @EuroNanoLab.

This work was conducted within the Technologies for Sustainability Flagship of the Istituto Italiano di Tecnologia.

References

[1] P. Benoit, Energy for Development, 2019.
[2] S.E. Skilhagen, J.E. Dugstad, R.J. Aaberg, Desalination 220 (2008) 476–482.
[3] A. Cipollina, G. Micale, A. Tamburini, M. Tedesco, L. Gurreri, J. Veerman, S. Grasman, A. Cipollina, G. Micale (Eds.), Sustainable Energy from Salinity Gradients, Elsevier, 2016, pp. 135–180.
[4] N.Y. Yip, D. Brogioli, H. Hamelers, K. Nijmeijer, Environ. Sci. Tech. 50 (2016) 12072–12094.
[5] D. Brogioli, R. Ziano, R.A. Rica, D. Salerno, F. Mantegazza, J. Colloid Interface Sci. 407 (2013) 457–466.
[6] D. Brogioli, Phys. Rev. Lett. 103 (2009) 1–4.
[7] D. Brogioli, R. Ziano, R.A. Rica, D. Salerno, O. Kozynchenko, H. Hamelers, F. Mantegazza, Energy Environ. Sci. 5 (2012) 9870–9880.
[8] A. Siekierka, K. Smolińska-Kempisty, M. Bryjak, Desalination 495 (2020) 114670.
[9] M.C. Hatzell, M. Raju, V.J. Watson, A.G. Stack, A.C. van Duin, B.E. Logan, Environ. Sci. Technol. 48 (2014) 14041–14048.
[10] R.A. Rica, D. Brogioli, R. Ziano, D. Salerno, F. Mantegazza, J. Phys. Chem. C 116 (2012) 16934–16938.
[11] B.B. Sales, M. Saakes, J.W. Post, C.J. Buisman, P.M. Biesheuvel, H.V. Hamelers, Environ. Sci. Technol. 44 (2010) 5661–5665.
[12] F. La Mantia, M. Pasta, H.D. Deshazer, B.E. Logan, Y. Cui, Nano Lett. 11 (2011) 1810–1813.
[13] B. Yang, J. Yu, T. Ma, J. Mater. Chem. A 11 (2023) 3388–3398.
[14] K. Smolinska-Kempisty, A. Siekierka, M. Bryjak, Desalination 482 (2020) 114348.
[15] A. Pedico, D. Molino, P. Zaccagnini, S. Bocchini, V. Bertana, A. Lamberti, Adv. Sustain. Syst. 8 (2024) 2400106.
[16] K. Sharma, Y.-H. Kim, S. Yiacoumi, J. Gabitto, H.Z. Bilheux, L.J. Santodonato, R. T. Mayes, S. Dai, C. Tsouris, Renew. Energy (2016) 249–260.
[17] B. Lobato, S. Flores, L. dos Santos-Gomez, A. Garcia, A. Pernia, M. Prieto, M. Busto, A. Arenillas, Nanomaterials 14 (2024) 2031.
[18] M. Nasir, Y. Nakanishi, A. Patmonoaji, T. Suekane, Renew. Energy 155 (2020) 278–285.
[19] X.-W. Han, W.-B. Zhang, M.M. Theint, X. Zhou, J.-J. Li, J. Long, Renew. Energy (2023) 119288.
[20] X. Hu, X. Bao, M. Zhang, S. Fang, K. Liu, J. Wang, R. Liu, S.H. Kim, R.H. Baughman, J. Ding, Adv. Mater. 35 (2023) 2303035.
[21] H. Wang, M. Shi, K. Zhu, Z. Su, X. Cheng, Y. Song, X. Chen, Z. Liao, M. Zhang, H. Zhang, Nanoscale 8 (2016) 18486–18494.
[22] S.H. Kim, C.S. Haines, N. Li, K.J. Kim, T.J. Mun, C. Choi, J. Di, Y.J. Oh, J.P. Oviedo, J. Bykova, S. Fang, N. Jiang, Z. Liu, R. Wang, P. Kumar, R. Qiao, S. Priya, K. Cho, M. Kim, M.S. Lucas, L.F. Drummy, B. Maruyama, D.Y. Lee, X. Lepro, E. Gao, D. Albarq, R. Ovalle-Robles, S.J. Kim, R.H. Baughman, Science. 357 (2017) 773–778.
[23] J.L. Blackburn, A.J. Ferguson, C. Cho, J.C. Grunlan, Adv. Mater. 30 (2018) 1704386.
[24] D. Feng, B. Zhou, P. Li, C. Liu, R. Elgamal, G. ElMasry, T. Zhang, Y. Feng, Renew. Energy (2025) 123846.
[25] M.S. Misenan, M.S. Ahmad Farabi, Z.N. Akhlisah, A.S. Khiar, Next Mater. 7 (2025) 100365.
[26] S. Ghosh, A.K. Sood, N. Kumar, Science. 299 (2003) 1042–1044.
[27] R. Kumar, T. Tabrizizadeh, S. Chaurasia, G. Liu, K. Stamplecoskie, Sustain. Energy Fuels 6 (2022) 1141–1147.
[28] Y. Kunai, A.T. Liu, A.L. Cottrill, V.B. Koman, P. Liu, D. Kozawa, X. Gong, M. S. Strano, J. Am. Chem. Soc. 139 (2017) 15328–15336.
[29] B. Shkodra, M. Petrelli, M.A. Angeli, D. Garoli, N. Nakatsuka, P. Lugli, L. Petti, Appl. Phys. Rev. 8 (2021) 041325.
[30] I.D. Rosca, F. Watari, M. Uo, T. Akasaka, Carbon 43 (2005) 3124–3131.
[31] J. Dangbegnon, N. Garino, M. Angelozzi, M. Laurenti, F. Seller, M. Serrapede, P. Zaccagnini, P. Moras, M. Cocuzza, T. Ouisse, H. Pazniak, J. Gonzalez-Julian, P. M. Sheverdyaeva, A. Di Vito, A. Pedico, C.F. Pirri, A. Lamberti, J. Energy Storage 63 (2023) 106975.
[32] F. Liu, R.M. Wagterveld, B. Gebben, M.J. Otto, P.M. Biesheuvel, H.M. Hamelers, Colloid inter, Sci. Commun. 3 (2014) 9–12.
[33] A.V. Delgado, S. Ahualli, M.M. Fernandez, M.A. Ganzalez, G.R. Iglesias, J.F. Vivo-Vilches, M.L. Jimenez, Environ. Chem. 14 (2017) 279–287.
[34] V. Obreja, Phys. E Low-dimens. Syst. Nanostruct. 40 (2008) 2596–2605.
[35] J. Li, M. Ostling, Crystals 3 (2013) 163–190.
[36] M. Serrapede, F. Seller, P. Zaccagnini, M. Castellino, I. Roppolo, F. Catania, J. Tata, T. Serra, S. Bianco, A. Lamberti, Carbon 213 (2023) 118283.
[37] P. Censi, S. Mazzola, M. Sprovieri, A. Bonanno, B. Patti, R. Punturo, S.E. Spoto, F. Saiano, G. Alonzo, Chem. Ecol. 20 (2004) 323–343.
[38] M.M. Salama, S.K. El Ebaidi, D.P. Stickley, in: 13th International Conference on Materials Science and Its Applications in Oil and Gas Industries, Benghazi, 2013, pp. 172–192.
[39] T.I. Shaw, L.H. Cooper, Nature 180 (1957) 250.
[40] F. Scholz, C. Hensen, G.J. De Lange, M. Haeckel, V. Liebetrau, A. Meixner, A. Reitz, R.L. Romer, Geochem. Cosmochim. Acta 74 (2010) 3459–3475.
[41] N. Koron, J. Faganeli, I. Falnoga, D. Mazej, K. Klun, N. Kovac, Mar. Chem. 157 (2013) 185–193.
[42] P.L. Runnels, J.D. Joseph, M.J. Logman, R.M. Wightman, Anal. Chem. 71 (1999) 2782–2789.
[43] A. Atchabarova, S. Abdimomyn, D. Abduakhytova, Y. Zhigalenok, R. Tokpayev, K. Kishibayev, T. Khavaza, A. Kurbatov, Y. Zlobina, T. Djenizian, J. Electroanal. Chem. 922 (2022) 116707.
[44] M. Thommes, K. Kaneko, A.V. Neimark, J.P. Olivier, F. Rodriguez-Reinoso, J. Rouquerol, K. Sing, Pure Appl. Chem. 87 (2015) 1051–1069.
[45] F. Liu, T.F. Donkers, M.R. Wagterveld, O. Schaetzle, M. Saakes, C.J. Buisman, H. V. Hamelers, Electrochim. Acta 187 (2016) 104–112.
[46] F. La Mantia, M. Pasta, D. Brogioli, A. Cipollina, G. Micale (Eds.), Sustainable Energy from Salinity Gradients, Elsevier, 2016, pp. 1–48.
[47] F. Liu, O. Schaetzle, B.B. Sales, M. Saakes, C.J.N. Buisman, H.V.M. Hamelers, Energy Environ. Sci. 12 (2012) 8642–8650.
[48] D.G. Kim, D. Kim, H. Kim, H. Seo, H. Choi, Y.-G. Jung, G.S. An, J. Choi, H. Kim, S. Myeong, Y. Jung, D. Lee, I. Hwang, T. Song, S. Yang, Desalination 556 (2023) 116574.
[49] Z. Zou, L. Liu, S. Meng, X. Bian, Energy Rep. 8 (2022) 7325–7335.
[50] M.G. Busto, M.J. Prieto, J.A. Martin-Ramos, J.A. Martinez, A.M. Pernia, Electronics 13 (2024) 42.